INL/JOU-20-60791-Revision-0

Cost- and Risk-Based Seismic Design Optimization of Nuclear Power Plant Safety Systems

August 2021

Changing the World's Energy Future

Chandrakanth Bolisetti, Justin L Coleman, Andrew Whittaker, William M Hoffman

Idaho National Laboratory

INL/JOU-20-60791-Revision-0

Cost- and Risk-Based Seismic Design Optimization of Nuclear Power Plant Safety Systems

Chandrakanth Bolisetti, Justin L Coleman, Andrew Whittaker, William M Hoffman

August 2021

Idaho National Laboratory
Idaho Falls, Idaho 83415

http://www.inl.gov

Prepared for the
U.S. Department of Energy
Under DOE Idaho Operations Office
Contract DE-AC07-05ID14517

Cost- and Risk-Based Seismic Design Optimization of Nuclear Power Plant Safety Systems

Chandrakanth Bolisetti,[a*] Justin Coleman,[a] William Hoffman,[a] and Andrew Whittaker [b]

[a]*Idaho National Laboratory, Advanced Reactor Design and Deployment, Idaho Falls, ID*

[b]*University at Buffalo, State University of New York, Civil, Structural, and Environmental Engineering, Amherst, NY*

*Corresponding author

Email: chandrakanth.bolisetti@inl.gov

Phone: +1 716-352-5107

Cost- and Risk-Based Seismic Design Optimization of Nuclear Power Plant Safety Systems

Seismic analysis, design, and qualification of systems, structures, and components (SSCs) is a significant contributor to the capital cost of a nuclear power plant. To reduce capital costs of advanced nuclear power plants and make commercial nuclear energy more competitive, innovations are needed in their structural design and construction, and not just in the reactor core and associated systems. Seismic isolation has been identified as an important cost-cutting technology that enables standardization of equipment across various sites. This paper develops and demonstrates a cost- and risk-based seismic design optimization of a representative safety system in a nuclear power plant with the dual goals of minimizing overnight capital cost and meeting safety goals. The design optimization can also include component seismic isolation, in which case, the optimized design includes a set of equipment that need to be seismically isolated to minimize capital cost. The open-source codes MASTODON and Dakota are used for seismic probabilistic risk assessment (SPRA) and design optimization, respectively. A generic nuclear facility with a safety system comprising SSCs that are common to nuclear power plants is considered for the demonstration of the design optimization and is assumed to be located at the Idaho National Laboratory site. Generic costs and seismic design cost functions are assumed for the SSCs of the safety system. The sum of the costs of the SSCs is minimized in the optimization process, while the risk of failure of the safety system is provided as a constraint. Results show that the optimization process reduces capital costs significantly while automatically prioritizing the safety of SSCs that contribute most to the risk of the safety system.

Keywords: design optimization; seismic design; seismic probabilistic risk assessment; balance-of-plant design; advanced reactors

I INTRODUCTION

The nuclear industry in the United States is currently at a severe economic disadvantage, mainly due to the large capital cost of new nuclear power plants (NPPs). Recent NPP construction projects have seen large cost overruns and schedule delays, making the commercial nuclear sector unattractive to investors. To minimize the effects of climate change over the coming decades, it is important to replace fossil fuels plants with low-carbon, high-reliability energy sources like nuclear power plants not only in the United States, but also in other countries including many developing countries like India, China, and African nations, which currently rely heavily on coal and natural gas to generate electricity. Advanced reactor concepts currently under development in the United States [e.g., the High Temperature Gas Reactor (HTGR) of X-Energy, Fluoride-Salt-Cooled High Temperature Reactor of Kairos Power (KP-FHR), NATRIUM™ reactor of TerraPower and GE Hitachi, and the Molten Chloride Fast Reactor (MCFR) of TerraPower] are striving to improve the economics of nuclear power primarily by using passive and 'walk-away' safe reactor technologies and substantially reducing the number of safety systems. Recent studies[1,2,3] have found that a significant contributor to the capital cost of NPPs is the 'civil works', that is, the construction of the balance of plant (BoP: all systems, structures, and components except those involved in power generation, e.g., reactor vessel) such as the buildings, containment dome, foundation, etc., which amount to almost half of the overnight capital cost. They also identify seismic design as an important contributor to the capital costs, because of the highly site dependent nature of seismic hazard. Buongiorno et al.[1] provide recommendations to reduce capital costs including improvements in construction management practices, adoption of advanced technologies that reduce on-site construction (steel composite walls and segmented, precast reinforced concrete construction) and promote design standardization (e.g., seismic isolation), all of which can result in significant reduction in capital costs and time to construct. The study presented in this paper proposes another means for capital cost reduction: design optimization. Design optimization is a routine goal of all branches of engineering. For example, the designs of some buildings, commercial airliners, fighter jets, and automobiles are optimized to reduce the cost of fabricating or constructing each product, within the constraints of safety, regulations, and manufacturability. Because of the disciplines involved, the design optimization of a nuclear power plant (NPP) can be considerably more complex, given the stringent regulations in the nuclear industry and the disparate collection of a large number of systems, structures and components (SSCs), including structural elements, and mechanical and electrical equipment, that comprise each NPP.

Although advanced reactors are designed with passive safety systems, the seismic design procedures for the balance of plant (BoP) of these reactors are similar to those used in existing nuclear power plants. Without swift and aggressive innovation in these design procedures and construction technologies aimed towards reducing capital costs, advanced reactors are at a risk of being too expensive. In addition to increased safety, risk reduction from advanced reactor technologies provides a unique opportunity to optimize design and reduce capital costs, especially in the BoP. Traditionally, nuclear power plants have been designed using deterministic, non-iterative methods that result in conservative and expensive designs. These design procedures do not employ capital cost as a design selection criterion and only rely on safety (risk) and performance. Additionally, each component in the facility is designed individually to achieve a required seismic capacity, and the interdependence between the components in ensuring plant safety is not typically considered in design[4,5]. As a result, risk reduction from better safety features in one component or a system cannot be leveraged to reduce conservatisms in other components, even though they function together to ensure plant safety. Recently, the Nuclear Regulatory Commission (NRC) has sponsored the development of a risk-informed performance-based (RIPB) regulatory framework[4,6] for seismic safety that aims to improve the seismic design and licensing of advanced non-light water reactors (LWRs). This framework stems from the nuclear industry-led and NRC-endorsed Licensing Modernization Project[7,8] (LMP), which developed a technology inclusive risk-informed and performance-based (TI-RIPB) process for the selection of licensing basis events (LBEs) and safety classification of SSCs for non LWRs. The RIPB framework, which is separate from the TI-RIPB process of the LMP and focuses specifically on seismic design, aligns with the existing American Society of Civil Engineers (ASCE) seismic design standard (ASCE 43-19[5]) and integrates seismic probabilistic risk assessment (SPRA) into the design process. This RIPB framework along with the LMP are the first to provide qualitative guidance on making design decisions that may reduce capital cost while ensuring safety and performance. Both the LMP and the RIPB framework were under development at the time of writing of this paper and therefore, are not integrated into the study presented in this paper. While this is an evolving regulatory environment that is poised to become more flexible, very few research studies (e.g., Schumock et al.[9], Wang and Lin[10], Kwag and Hahm[11]) have been undertaken that use both cost and risk as seismic design criteria. This is partly due to the lack of data that describes the change in capital cost with design parameters, making it challenging to explicitly account for cost in design. Stevenson[12] performed a cost analysis of existing reactors and provided empirical relationships between the design peak ground acceleration (PGA) and the capital costs of various classes of SSCs (e.g., distribution systems, mechanical systems, etc.). Yu et al.[13] used this data to characterize the economic benefits of seismic isolation of a generic nuclear facility in the DOE complex. The lack of data for advanced reactors is being remedied by Lal et al.[14,15], who are developing functional relationships between the design seismic intensity and the cost 'penalty' (i.e., capital costs incurred for the seismic design beyond a nominal design level) for a selection of safety components in advanced reactors.

This study proposes an iterative risk- and cost-based design process in which, the seismic design is optimized to both meet safety performance goals, as well as to minimize the total capital cost. This design process is termed as risk- and cost-based design optimization. While this design optimization process is not expected to replace the current, deterministic seismic design process of ASCE 43 or the RIPB process it is intended to equip designers perform 'intelligent' early-stage design iterations that replace manual iterations and enable them to make design decisions such as the use of seismic isolation or the choice of the plant layout, which can also significantly impact seismic design. This paper describes the development of the risk- and cost-based seismic design optimization and demonstrates it for an idealized, but representative, safety system in a nuclear facility, hereafter referred to as the generic nuclear facility (GNF). The GNF is assumed to be sited at the Idaho National Laboratory (INL) site, which has a low-to-moderate seismic hazard. The design of the safety system in GNF is defined by seismic fragilities of the SSCs in the safety system. Seismic fragility is a measure of the seismic capacity of the SSC and is represented as a double lognormal distribution defined by a median and two lognormal standard deviations for epistemic and aleatory uncertainties[16]. For a higher median fragility, the seismic integrity of the SSC is higher, and seismic risk is smaller. A higher seismic fragility also requires more upfront capital investment either to retrofit the SSC or to demonstrate a higher seismic capacity (e.g., through additional qualification and testing) and therefore has a higher capital cost. The goal of the design optimization process presented in this paper is to minimize the total capital cost of the GNF while meeting performance goals, which are to remain below a user-specified seismic risk limit. This is an optimization problem involving capital cost and risk calculation for the safety system during each iteration. The seismic risk is calculated through seismic probabilistic risk assessment (SPRA) involving fault tree and event tree analyses (FTA and ETA) performed using MASTODON[17,18], which is an open-source seismic analysis and risk assessment software being developed at the Idaho National Laboratory. The optimization is performed using Dakota[19], which is another open-source software for optimization and uncertainty quantification developed at Sandia National Laboratory. Section II describes the SPRA process in MASTODON and Section III describes the formulation of the design optimization problem to be solved by Dakota. Section IV presents the development of a representative probabilistic risk assessment (PRA) model for the GNF and the capital cost calculation process for GNF. Section V describes the design optimization of GNF using MASTODON and Dakota along with the results. In this section, design optimization is first performed without including component seismic isolation, and the optimal seismic fragilities are calculated that result in a minimum capital cost. The optimization is performed again while including component seismic isolation. In this case, in addition to calculating the optimal seismic fragilities, the design optimization process also results in the optimal set of SSCs that need to be seismically isolated to minimize the capital cost. Section **Error!**

Reference source not found. presents a summary and considerations for practical implementation of the optimization framework, and Section VI presents the conclusions.

II SEISMIC PROBABILISTIC RISK ASSESSMENT USING MASTODON

MASTODON performs SPRA calculations using the time-based methodology proposed by Huang, et al.[16]. This methodology (hereafter referred to as the Huang methodology) accommodates nonlinear response in the soil-structure system, unlike typical implementations of the traditional SPRA approach[20] that assume linear behavior throughout the model. The Huang methodology is therefore suitable for problems that include nonlinear soil-structure interaction (SSI), nonlinear site response, seismic isolation, and nonlinear structural response (which may occur in some advanced reactors during design basis shaking and in large light water reactors during beyond design basis shaking). A primary improvement in this methodology from the traditional SPRA is the usage of fragility curves for systems, structures and components (SSCs) that are functions of a local demand parameter such as, spectral acceleration at the point of attachment of the equipment. In a traditional SPRA approach, the SSC fragility curves are typically expressed as functions of peak ground acceleration (PGA).

The Huang SPRA methodology involves five steps, as illustrated in Figure 1. The first step is plant system analysis, which involves the development of event trees and fault trees that lead to an accident or an unacceptable event (such as core damage). Fault trees describe the logic leading to the occurrence of a top event from one or more basic events, which typically correspond to the damage or failure of an SSC, such as a pipe burst or a shear wall failure. For each of these basic events, a fragility curve is calculated, which describes the probability of the occurrence of the basic event conditioned upon a local demand parameter such as the story drift of a shear wall. An event tree describes the logic between several such top events leading to an accident or an unacceptable event. The second step involves a probabilistic seismic hazard analysis and the calculation of seismic hazard curves, which describe the mean annual frequency of exceedance (MAFE) of a particular ground motion parameter, such as PGA or the spectral acceleration at 0.1 sec. In the Huang methodology, the seismic hazard curve is divided into several intervals (or bins or stripes) spanning across the range of interest of the seismic hazard. Ground motions are selected and scaled for each of these bins such that they represent the seismic hazard of the bin as well as the uncertainty in the ground motion characteristics, such as frequency content. The third step involves probabilistic simulations of the structure using the ground motions selected in the previous step. These probabilistic simulations involve random sampling (using sampling procedures like Monte Carlo or Latin Hypercube) of the ground motions and properties of the soil-structure system and performing several (tens to hundreds) simulations. The results of these simulations are used to calculate the probabilistic demands (expressed as lognormal distributions) at the locations of SSCs corresponding to the basic events. In the Huang methodology, the demands from the tens or hundreds of simulations are expanded to hundreds of thousands of demands using the Yang, et al.[21] procedure, which conserves the statistical correlations between the various SSC demand distributions while expanding the demand datasets. The fourth step involves using these demands, along with the fragility curves calculated in the first step, to calculate the probability of failure of the SSCs conditioned upon the seismic demands. In the fifth step, these conditional probabilities of failure, along with the event trees and fault trees developed in the first step, are used to calculate the probability of occurrence of the accident or unacceptable event for each hazard bin. Such a calculation is referred to as fault tree analysis (FTA) and can be performed either using a closed-form solution, or through Monte Carlo simulations using the expanded demand datasets calculated in the previous step. Although the closed-form solutions are computationally inexpensive, they also assume that the demands from various SSCs are statistically independent. However, the Monte-Carlo simulations proposed by the Huang methodology do not require this assumption. Yu, et al.[13] compared the results calculated using the closed form solutions and Monte Carlo simulations for a simple fault tree and found that the results are similar for the problem considered in their study. The FTA is repeated for all the hazard bins of step 2 and the probability of each bin is multiplied with the corresponding mean annual frequency of shaking (from the hazard curve) to calculate the risk contribution from each bin. The total risk of accident or unacceptable performance is then calculated as the sum of the risk contributions.

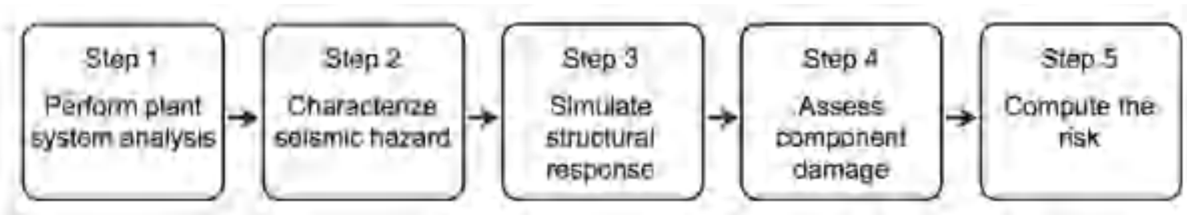

Figure 1: The SPRA methodology[16,22]

The Huang SPRA methodology is implemented in MASTODON, both as a Python module and as a part of the source code (written in C++). While the inclusion in the source code provides a continuous integration between the finite-element simulations and SPRA, the Python module provides the flexibility to perform standalone SPRA in a more interactive environment. Both the Python module and the source code offer the capability to perform steps 3, 4, and 5 of the Huang SPRA methodology illustrated in Figure 1. The integration of SPRA in MASTODON and a description of the capabilities is presented in Figure 2.

MASTODON inputs the ground motions selected and scaled in step 2 and uses the stochastic tools module of the MOOSE framework to sample the properties of the finite element model along with the ground motions and run probabilistic simulations. Currently, it includes the Latin Hypercube and Monte Carlo samplers and is capable of efficiently parallelizing the probabilistic simulations amongst hundreds or thousands of processors. MASTODON also inputs the number of bins in the hazard curve, and postprocesses the probabilistic demands at SSC locations for each of these bins. Using the fragility curves (or capacity distributions, i.e., the probability of failure of the SSC given a local demand parameter) for each SSC provided by the user, MASTODON then calculates a probability of failure conditioned upon seismic shaking for each bin. A lognormal distribution is fit into these probabilities of failure to calculate an ‘enhanced fragility’, which describes the probability of failure of the SSC conditioned upon the seismic input to the plant. These enhanced fragilities are then used in the FTA to calculate the system fragility. The system fragility is then convolved with the seismic hazard according to step 5 of the Huang SPRA methodology (and consistent with traditional approaches) to calculate the system risk.

Fault tree analysis and quantification in MASTODON can be performed both using closed-form solutions as well as Monte Carlo simulations. Currently, MASTODON is limited to the quantification of one fault tree at a time and does not analyze event trees. The closed-form solutions for FTA in MASTODON are calculated using the same approach used by the industry-standard probabilistic risk assessment (PRA) code, Saphire[23] developed by INL for the United States Nuclear Regulatory Commission (USNRC). Saphire uses the MOCUS (Method for Obtaining Cut Sets) algorithm [24,25] to perform FTA and calculate the minimal cut sets for each fault tree. A minimal cut set is a combination of basic events, which, when occur together, will lead to occurrence of the top event of the fault tree. Generation of cut sets using MOCUS is a recursive calculation involving various Boolean operations and application of set theory. A detailed description of this cut set generation procedure is provided in the Saphire technical manual[24]. Each fault tree can result in several minimal cut sets and the probabilities associated with these cut sets are calculated using the probabilities of basic events. This calculation is referred to as fault tree quantification. MASTODON, like Saphire, offers three methods of fault tree quantification: (1) rare event approximation, which involves the summation of the probabilities of all the minimal cut sets and is suitable for cut sets that have very small probabilities, (2) minimal cut set upper bound, which is an approximation of the probability of the union of all cut sets that provides a conservative estimate to the top event probability, and (3) min-max approach, which is an exact quantification of the fault tree and calculates the exact probability of the union of all the cut sets.

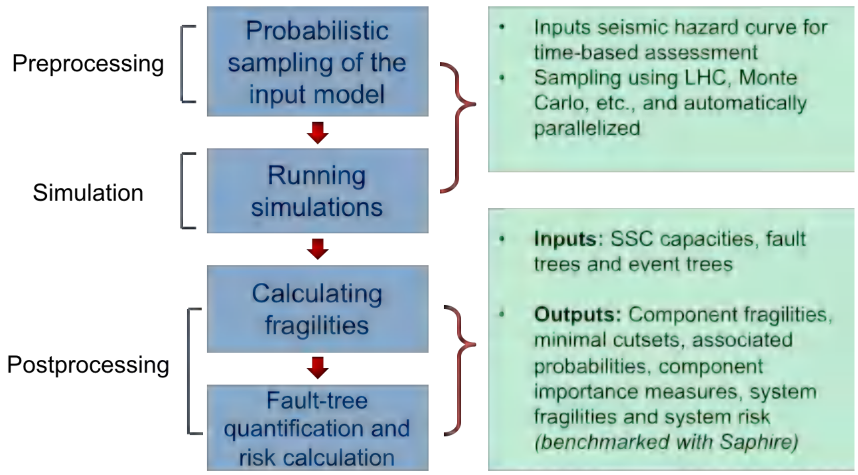

Figure 2: SPRA in MASTODON [17,26]

III FORMULATION OF THE RISK- AND COST-BASED DESIGN OPTIMIZATION PROBLEM

Mathematical optimization problems typically strive to minimize an objective function that depends on various design variables and subject to one or more constraints. The result of the optimization process is a set of design variables that result in the 'best' or minimum objective function while satisfying the constraints. In engineering practice, design optimization is typically used to calculate the set of design variables (e.g., geometry of the wing of an airplane) that maximizes the safety or efficiency of an engineering system while minimizing resources (e.g., amount of material). The objective of the design optimization described in this study is to minimize the total capital cost of a representative advanced reactor safety system, while keeping the risk of unacceptable performance below a user-specified threshold. The safety system is assumed to include several SSCs that are vulnerable to earthquake shaking, and each of these SSCs has a fragility curve that is assumed to be representative of its seismic capacity. For this study, the cost of each SSC is assumed to be a function of its median fragility. The total cost of the safety system is then calculated as the sum of the costs of the SSCs. The risk of failure of the safety system is calculated using SPRA as described in Section II, using the seismic hazard curve, fragilities of the SSCs, and the fault tree of the safety system. The optimization framework is currently intended to be used for fine-tuning the early stages of design when preliminary details such as approximate fragilities and cost functions, and preliminary structural response models are available. The framework is not expected to result in the final design, for which, code-based design guidelines will still need to be followed. In the current demonstration, for simplicity, it is assumed that (a) the SSCs are only designed to meet the performance goal of the system, that is, not exceeding a user-specified risk threshold, (b) the structural response, that is, the demand, does not change significantly when the seismic fragility is changed, and (c) in the set of feasible designs, the median fragilities have a lower bound and an upper bound that are determined by practical constraints specific to the SSC. The optimization problem is described mathematically by equations 1 and 2 below.

$$C(a_1, a_2, .. a_n) = \sum_{i=1}^{n} c_i(a_i) \tag{1}$$

$$\text{minimize } C(a_1, a_2, \ .. \ a_n)$$

$$\text{subject to the constraints: } \begin{cases} R(LN(a_1, \beta_1), LN(a_2, \beta_2), \ .. \ LN(a_n, \beta_n)\ ) \leq \mathrm{R_U} \\ l_1 \leq \ a_1 \leq \ u_1 \\ l_2 \leq \ a_2 \leq \ u_2 \\ .. \\ l_n \leq \ a_n \leq \ u_n \end{cases} \tag{2}$$

In these equations, $a_1, a_2, .. a_n$ are the median seismic fragilities (or capacities) of n SSCs of the safety system and are also the design variables of the optimization problem. The objective function, C, is total capital cost of the safety system expressed as the sum of individual SSC costs, $c_i(a_i)$. Each of the functions, $c_i(a)$, is a cost function, which is the capital cost of the SSC as a function of its median seismic fragility, a. The constraints of the optimization problem are described by equation 2. The first constraint describes the performance goal, where $LN(a_i, \beta_i)$ are the lognormal fragility functions with a_i and β_i being the median and lognormal standard deviation, respectively, R is the risk of the unacceptable performance of the safety system, and R_U is the user-specified risk threshold. The rest of the constraints describe the upper and lower bounds (l_i and u_i) on the design variables, that is, the median fragilities of the SSCs. As the fragilities of the SSCs are reduced, the total cost of the system decreases, but the risk of an unacceptable performance of the system increases, and beyond a certain point, will exceed the threshold. The optimization algorithm will result in an optimal set of SSC fragilities that result in minimum total cost, while maintaining the risk below the threshold.

Although the optimization problem described here is idealized, it can be easily extended to more practical scenarios by adding more design variables, more complex cost functions, or additional design constraints. For example, component seismic isolation can be considered by changing the cost and fragility functions by accounting for the additional capital cost due to isolation, and the corresponding reduction in the probability of failure due to the smaller seismic demands. This is described in Section V.D. The simplicity of the problem chosen here enables a clearer interpretation of the initial and optimized design, and the behavior of the optimization algorithm. A generalized form of the algorithm is illustrated in Figure 3 below. This figure shows a snapshot of each evaluation in the optimization process, which starts with a design candidate and involves the calculation of the capital cost (objective function) and the seismic risk (constraint) of the design. The optimization is performed in Dakota, the seismic risk (R) is calculated using SPRA in MASTODON, and the capital cost (C) is calculated using a standalone Python script. Section V.A describes the coupling between these software to perform the design optimization of this study.

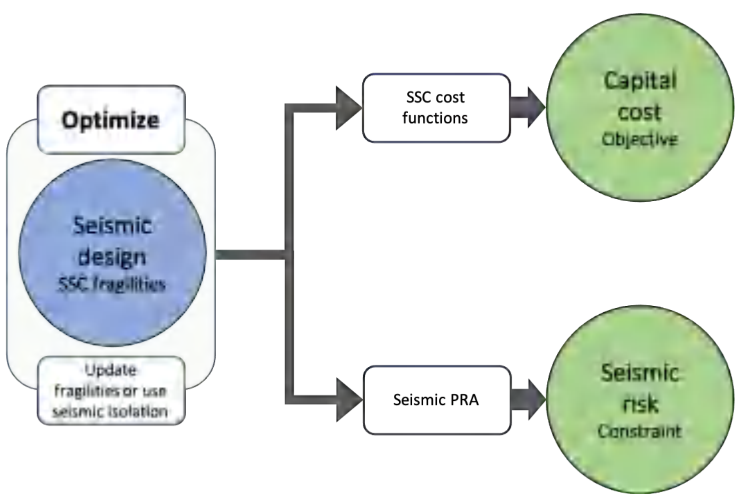

Figure 3: Illustration of the optimization problem of this study

Optimization algorithms can be broadly classified into gradient-based algorithms (e.g., gradient descent), which search for a local or global minimum of an objective function by moving along the gradient of the function, and non-gradient-based algorithms, which typically involve a logical and iterative search of the variable space, based on the value of the objective function and the adherence to the constraints of the optimization problem. Although gradient-based algorithms are fast, and often assure the best solution to a problem, they also require the objective functions to be continuous and differentiable. Engineering problems are often complex with a large number of design variables and constraints, and objective functions and constraints that are non-convex, not continuous or differentiable, or even expressible as mathematical functions. Moreover, design optimization problems often encounter discrete variables (e.g., thickness of a pressure vessel, which can only take discrete values, based on the thickness of metal plates that are rolled) or characteristic variables (e.g., a safety component being seismically isolated or not) and the problem can involve a combination of continuous and discrete variables, making it almost impossible to solve with traditional, gradient-based algorithms. Therefore, in the recent years, non-gradient-based approaches (sometimes labeled as nontraditional methods) have been increasingly employed for engineering problems. Non-gradient-based algorithms deploy numerically based, brute-force-type approaches that are slower than gradient-based counterparts and often search for the global optimum in a given design space. Although their use may not result in the mathematically optimal solution, they almost always converge to an engineering solution that is better than the initial solution, which by itself, is quite advantageous in engineering design optimization. Many non-gradient-based optimization algorithms are inspired by natural phenomena such as the behavior of biological or molecular systems. Examples include evolutionary or genetic algorithms, which are based on Darwin's theory of natural selection, and particle swarm optimization, which are based on the behavior of flocks of birds or schools of fish. Given their versatility and the widespread use, a genetic algorithm implementation in Dakota is used for this study. A detailed description of genetic or evolutionary algorithms can be found in the Dakota manual Adams, et al.[19], or various other sources such as Eddy and Lewis[27], Rao[28], etc.

IV DEVELOPMENT OF A GENERIC PRA MODEL FOR DESIGN OPTIMIZATION

IV.A Generic safety system

A safety system for a generic nuclear facility (GNF) that is adopted from Yu, et al.[13] and modified is used for this study. The GNF and the safety system are assumed to be representative of a range of nuclear reactor safety systems that comprise nuclear steam supply components including a reactor vessel, control rod drive mechanism (CRDM; or other reactor control or shutdown mechanisms), steam generator, coolant pump, and piping, electrical components including a motor control center (MCC) and a battery, and containment components including the containment structure, air handler and a duct. It is assumed that the failure of any of these component groups will lead to a failure of the safety system as described in the fault tree of Figure 4. The symbols, and in this figure represent AND and OR gates, respectively, and the circles denote basic events corresponding to the ten steam supply, electrical and containment components. The failure of the safety system in the GNF is assumed to cause unwanted release of radioactive material into the environment, as shown in the event tree presented in Figure 5. The SSCs considered here are representative of both existing and advanced nuclear reactor facilities and are taken from the Electric Power Research Institute (EPRI) SPRA Guide[20]. Note that this safety system is illustrative and not representative of any specific nuclear facilities.

The SPRA of this safety system is performed using the Python FTA module available in MASTODON[a]. Since the event tree only comprises a single event corresponding to the fault tree of the generic safety system, the success or failure of the fault tree also determines the success or failure in the event tree. Therefore, the system risk is calculated only using the fault tree quantification and not event tree quantification is performed. The GNF is assumed to be located within the boundary of the Idaho National Laboratory (INL) and the corresponding seismic hazard curve at a period of 0.1

[a] The MASTODON source code can be freely downloaded from the GitHub page, https://github.com/idaholab/mastodon, and the documentation can be found on the MASTODON website, https://mooseframework.inl.gov/mastodon.

sec, calculated by Yu, et al.[13] from United States Geological Survey (USGS) data, is used for this study. This seismic hazard curve is presented in Figure 6.

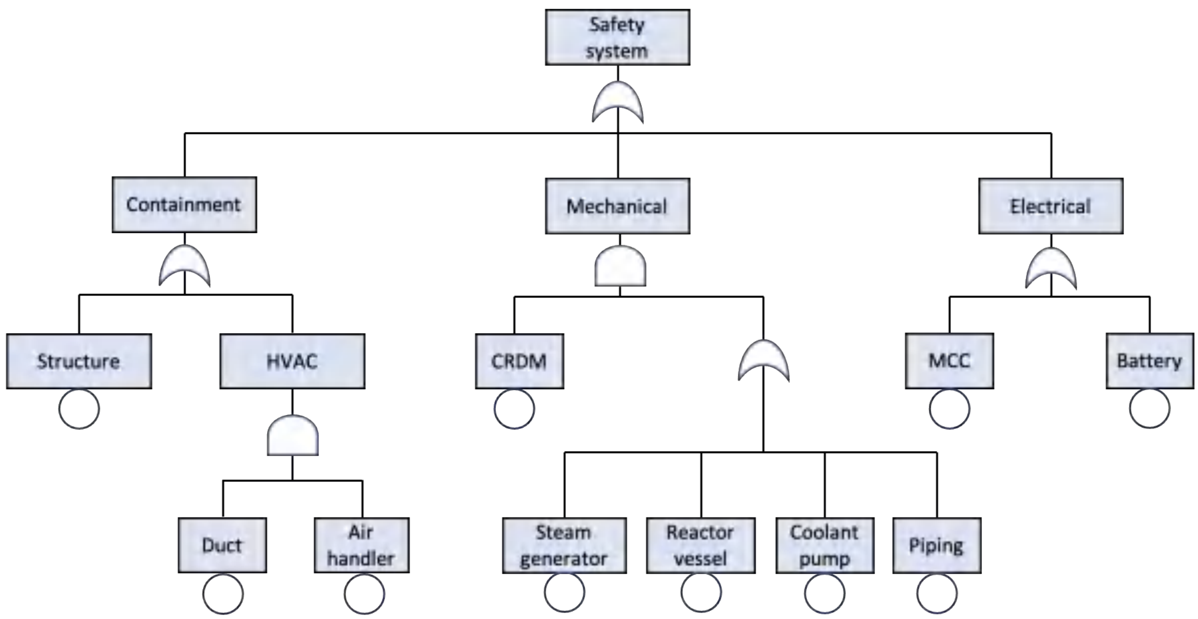

Figure 4: Fault tree[13]

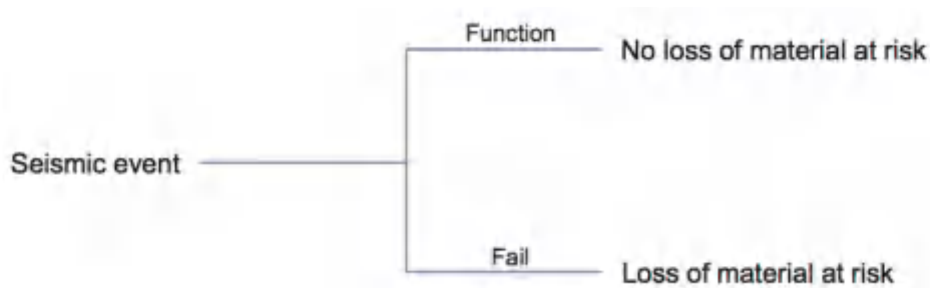

Figure 5: Event tree[13]

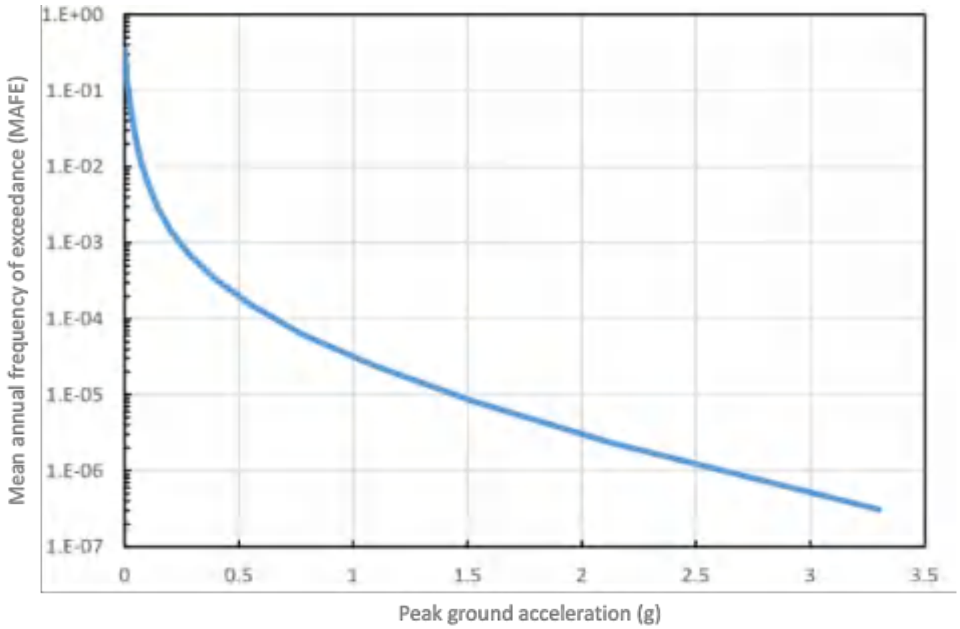

Figure 6: Seismic hazard curve for the peak ground acceleration at the INL site[13]

IV.A.1 Development of fragility and cost functions

The seismic design of the GNF safety system is characterized in this study by the set of fragilities for the selected SSCs. Generic fragilities of the SSCs (median, A_m, and lognormal standard deviations due to uncertainty and randomness, β_u and β_r, respectively) are chosen from the fragilities recommended by the EPRI SPRA guide[20]. The composite lognormal standard deviation, β_c, is calculated as the square root of the sum of the squares of β_u and β_r. These fragilities are assumed to be the 'enhanced fragilities' in the MASTODON implementation of the Huang SPRA methodology, and represent the probability of failure of the SSCs conditioned upon the intensity of shaking in the hazard curve. The optimization algorithm also requires SSC fragility ranges (described by the bounds, l_i and u_i in equation 2) as input. The fragility ranges provided in the EPRI SPRA guide are used for this purpose and assumed to be sufficient for the purpose of this study. The initial fragilities for all SSCs in the GNF are listed in Table I.

Optimization of the seismic design of the safety system also requires estimates of costs of the SSCs as well as estimates of the increase of their costs with an increase in the seismic fragilities (i.e., the cost penalty for seismic design). A previous review of available literature by Bolisetti, et al.[29] and

Yu, et al.[13] found that public information regarding the seismic design costs in NPPs is scarce. The only publicly available information is through surveys conducted by Stevenson[30] on Generation II large light water reactors in the 1980s, and anecdotal information from experienced professionals in the nuclear industry. Lal et al.[14,15] and EPRI[31] generate and present data on the seismic design cost penalty for some critical pieces of equipment (reactor vessel, steam generator, and control rod drive mechanism) for incremented levels of ground shaking. Due to the lack of modern data for the SSCs in GNF, generic SSC costs and cost functions (variation of SSC costs with median fragilities) are assumed for this study. The SSC costs are adjusted such that the total capital cost of the initial design amounts to almost $100 million. To ensure that the optimization process works for a diverse set of cost function types, various functions including linear, step, quadratic and square root functions, are assumed for the different SSCs. These SSC cost functions are plotted for the fragility ranges of SSCs presented in Table I and are presented in Figure 7. Step functions are assumed to describe the cost increases with median fragility of the motor control center (MCC), batteries, and the coolant pump. A linear function is assumed for the air handler, reactor vessel, steam generator and the CRDM. Quadratic functions are assumed for the structure and the reactor vessel. The cost of the distribution systems, piping and ducts, is assumed to be directly proportional to the square root of the median fragilities, as suggested by Stevenson[30]. The cost increases (ratio of the maximum to minimum costs for a specific SSC presented in Figure 7) for the reactor vessel, steam generator, and the CRDM are chosen to be roughly the same as those presented in Lal et al.[14]. The total capital cost and seismic risk of the initial design are calculated and presented in Section IV.A.2.

Table I: List of SSCs in the GNF

SSC name	Initial median fragility* (g)	Lower bound* (g)	Upper bound* (g)	β_c^
MCC	2.0	1.0	2.9	0.46
Battery	1.5	1.0	2.0	0.46
Coolant pump	2.5	1.8	3.2	0.50
Air handler	2.5	2.0	4.0	0.50
Duct	2.0	1.0	3.0	0.61
Structure	2.0	1.6	2.4	0.46
Reactor vessel	2.0	1.0	3.0	0.46
Steam generator	2.5	1.5	4.0	0.58
CRDM	2.0	1.0	6.0	0.58
Piping	2.5	1.5	4.0	0.58

* Fragilities are defined in terms of peak ground acceleration

^ Composite lognormal standard deviation

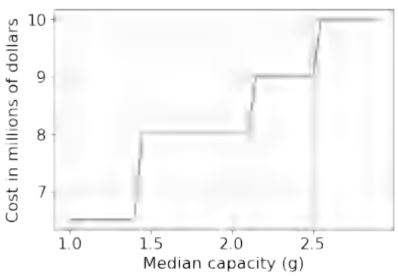

a. MCC

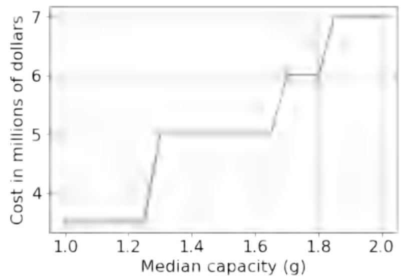

b. Battery

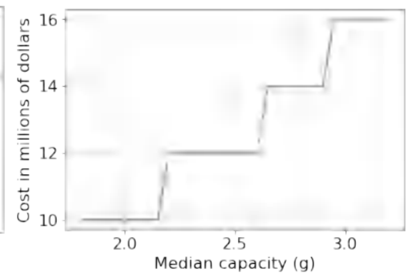

c. Coolant pump

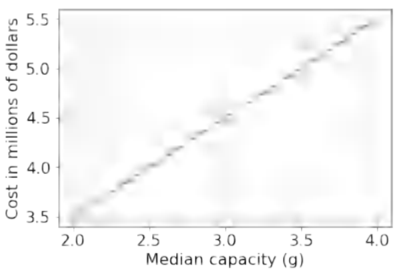

d. Air handler

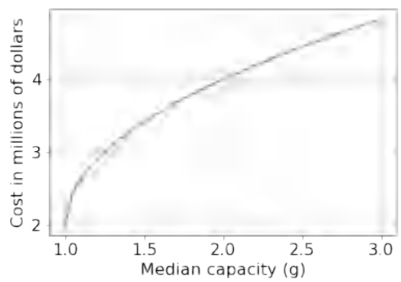

e. Duct

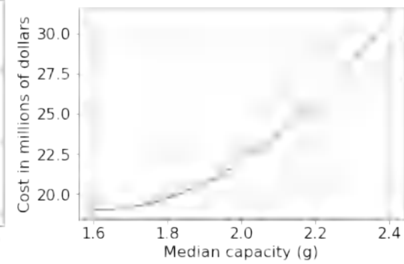

f. Structure

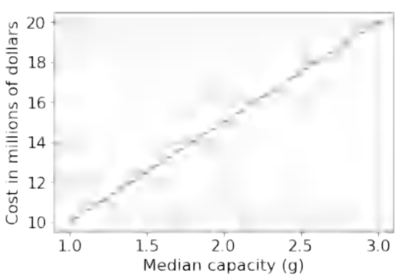

g. Reactor vessel

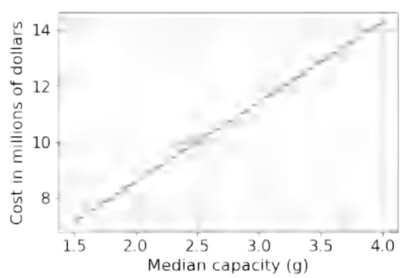

h. Steam generator

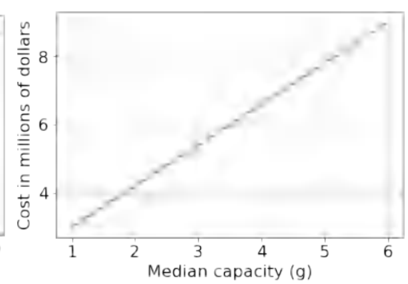

i. CRDM

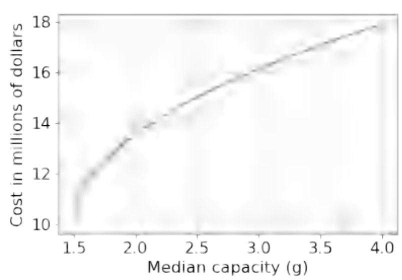

j. Piping

Figure 7: Capital costs of individual SSCs as a function of their median seismic fragility

IV.A.2 Capital cost and seismic risk of the initial design of the generic safety system

The initial capital cost of GNF calculated using the median fragilities in Table I and the cost functions in the Figure 7 is \$99.2 million. For simplicity, the risk calculation in the optimization of this study only involves steps 4 and 5 of the Huang methodology. Since the SSC fragilities are assumed to be functions of the shaking intensity in the hazard curve (PGA in this case), structural response simulations are not performed. Nevertheless, given the modular implementation of the PRA process in MASTODON, this procedure can be easily extended to include the structural simulations and perform a more comprehensive optimization. The hazard curve is split into ten bins, and the fault tree analysis and quantification are performed using the MOCUS method. For each bin, the probability of system failure is calculated and multiplied by the corresponding mean annual frequency to calculate the risk. The total system risk is then calculated as the sum of the risk in each of the ten bins. It is assumed that the performance goal of the GNF safety system is to stay under a risk limit of 5.0×10^{-5}. The system risk of the initial, unoptimized design of GNF calculated using MASTODON is 5.2×10^{-5}, roughly meeting the performance goal. This upper limit on the seismic risk of 5.0×10^{-5} is provided as a constraint to Dakota (R_U in equation 2). Seismic probabilistic risk assessment in MASTODON also results in the minimal cutsets and the corresponding risk contributions in the final risk. The minimal cutsets, corresponding risks and relative risk contributions are presented in Table II. The abbreviations listed in the table are used to denote the minimal cutsets in the results presented in Section V.

Table II: Minimal cutsets of the GNF safety system* and their corresponding risks in the initial design

Minimal cutset	**Abbreviation**	**Risk**	**Risk contribution (%)**
Structure	‘struct’	9.3×10^{-6}	18
MCC	‘mcc’	9.3×10^{-6}	18
Battery	‘batt’	2.3×10^{-5}	45
Air handler AND Duct	‘airhand & duct’	1.7×10^{-6}	3
Steam generator AND CRDM	‘sgen & crdm’	2.0×10^{-6}	4
Reactor vessel AND CRDM	‘pvess & crdm’	2.7×10^{-6}	5
Coolant pump AND CRDM	‘cpump & crdm’	1.7×10^{-6}	3
Piping AND CRDM	‘piping & crdm’	2.0×10^{-6}	4
Total risk		$\mathbf{5.2 \times 10^{-5}}$	**100.00**

V DESIGN OPTIMIZATION OF THE GENERIC SAFETY SYSTEM

V.A Coupling MASTODON and DAKOTA

Dakota offers optimization capabilities using genetic algorithms through the 'JEGA' package implemented by Eddy and Lewis[27]. This package includes the single-objective genetic algorithm (SOGA) and multi-objective genetic algorithm (MOGA), which are offered in Dakota as separate algorithms. The SOGA method is used for the design optimization of this study. This method can optimize both constrained and unconstrained problems, and can accommodate continuous, discrete, and characteristic design variables. Dakota provides interfaces to couple with external software, which can compute and provide objective functions, constraint functions, gradient matrices or the Hessian matrices. For this study Dakota, MASTODON, and the Python script for capital cost calculation are coupled through Dakota's 'fork' interface. This interface is a Python file that transfers iterated design variables from Dakota to MASTODON (which calculates the seismic risk, i.e., the constraint value in equation 2 using fault tree and event tree analysis) and the calculated constraint value back to Dakota. The interface also transfers the iterated design variables to the Python script for capital cost evaluation (i.e., the objective function in equation 1), which is again transferred back to Dakota.

V.B Sensitivity of the results to the genetic algorithm parameters

The Dakota input file includes the fragility ranges and Boolean values for seismic isolation for all SSCs, specification of the objective function and the risk constraint, and as well as the SOGA optimization parameters including population size, number of iterations, seed value for randomization, and crossover, mutation, and replacement types. While Dakota offers choices for the crossover, mutation, and replacement types, the default types are chosen for this study as recommended by the Dakota manual[19]. Prior to performing the design optimization of the safety system of GNF, the sensitivity of the results (i.e., the final objective function and the constraint, which are the capital cost and the seismic risk of the optimized design) to the seed value and population size is examined in this section. Additionally, the convergence of the solution with number of iterations is also examined. The sensitivity analysis is performed for the safety system of GNF, with the seismic hazard, event tree and fault tree, median fragility ranges and cost functions provided in Section IV. Seismic isolation is not considered for the sensitivity analyses.

Any stochastic study involving randomization involves a seed value that is used for random number generation. In SOGA, for example, the initial population is generated by randomly sampling the design space. The seed value ensures that the randomization, and therefore, the optimization is repeatable, that is, the same result is calculated when the optimization is repeated with the same seed. However, when different seed values are used, the algorithm is likely to produce different results and to ensure stability, these differences must be small. Table III presents the total capital cost and seismic risk of the optimized design with four different seed values. The table shows that the results are almost the same for all four seed values. The seismic risk of the optimized design is slightly smaller than the constraint, which is 5.0×10^{-05}, for all seed values, and the total capital cost of the optimized design is consistently around $83 million USD, which is about 16% smaller than that of the initial, unoptimized design. These results demonstrate the stability of SOGA with a changing seed value. The optimization results are discussed in more detail in Section V.C.

Another important parameter in SOGA is the population size. A population size that is too small may not adequately cover the design range and may result in a suboptimal solution. A very large population size will lead to solution that is a theoretical optimum but will require more function evaluations and longer computation time. To choose a reasonable population size five optimization analyses are performed with increasing population sizes. Table IV presents the total capital cost and the seismic risk of the optimized design for different population sizes, along with the total number of function evaluations required to reach an optimum. The table shows that for a small population size (10) the total capital cost of the optimized design is around $89 million, which reduces to around $83 million for a population size of 50. The results show that the optimized solution converges with increasing population size.

The optimization analyses performed so far involved 40 iterations, that is, 40 generations of the SOGA populations. Figure 8 presents a scatter of the capital cost (objective function) and seismic risk (constraint) of SOGA population at various stages of the optimization process when a seed of 30 and a population size of 50 is chosen. The blue triangle in the figure corresponds to the initial, unoptimized design and the orange circles correspond to the various designs in the population. The figure presents these values for iterations 1, 10, 25, and 40 and illustrates the convergence of the population to one single point, which is the optimal solution. The figure therefore shows that the algorithm converges to an optimal solution with repeated iterations and that 40 iterations is adequate for the current problem.

Although the algorithm is stable and convergent for the parameters calculated in this section, these parameters are specific to the problem presented here. The sensitivity analysis presented in this section should be repeated for each new problem and the appropriate genetic algorithm parameters should be calculated in order to achieve the best results.

Table III: Sensitivity of the optimization results to the randomization seed for SOGA

Seed	**Seismic risk from optimized design**	**Capital cost of optimized design (USD millions)**
10	5.0×10^{-5}	83.3
20	4.9×10^{-5}	84.2
30	5.0×10^{-5}	83.2
40	5.0×10^{-5}	83.9

Table IV: Sensitivity of the optimization results to the population size

Population size	**Seismic risk from optimized design**	**Capital cost of optimized design (USD millions)**	**Total number of function evaluations**
10	5.0×10^{-5}	88.8	136
20	5.0×10^{-5}	83.9	632
30	4.8×10^{-5}	83.9	772
40	5.0×10^{-5}	83.6	1326
50	5.0×10^{-5}	83.2	1395

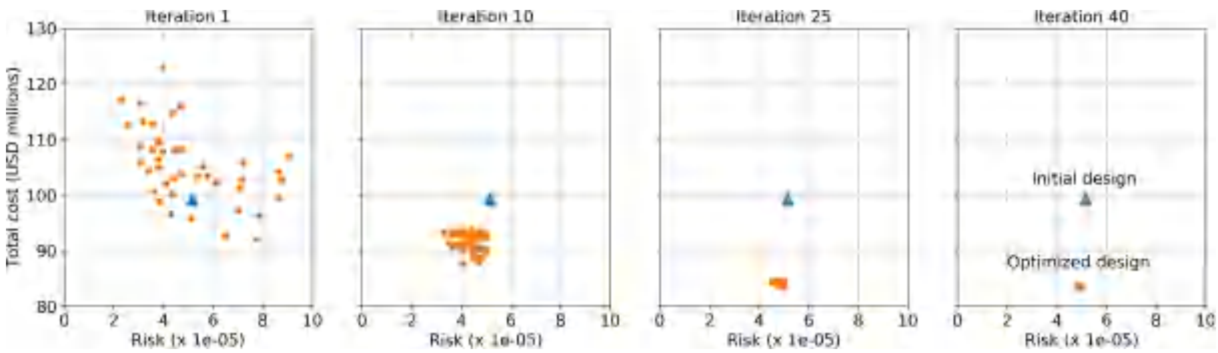

Figure 8: Convergence of the total capital cost with number of iterations in SOGA

V.C Design optimization of the safety system without component seismic isolation

Results of the design optimization are presented in this section, including the median fragilities of the SSCs that result in the minimal capital cost and meeting the risk target of 5.0 x 10^{-5}. Component isolation is not included as an option in the optimization process here and is considered in Section V.D. Detailed instructions for running the optimization problem including the input files, post processing files, and results are reproduced as a MASTODON example, which is available on the MASTODON documentation website. As shown in the Dakota input file, a population size of 50, seed value of 30, and a maximum number of iterations (generations) of 40 are chosen for design optimization of the GNF safety system based on the sensitivity analyses presented in Section V.B. Additionally, default parameters are used for the replacement, crossover, and mutation parameters, including the crossover and mutation rates of 0.8 and 0.08, respectively. The fragility range of each SSC listed in Table I are also provided in the Dakota input file. For each design fitness evaluation, the objective function (total cost) and the constraint (risk) are calculated in the Python interface file by calling the cost function file and the MASTODON PRA module, respectively. Apart from the median fragilities, which are the design variables, the seismic hazard shown in Figure 6, lognormal standard deviations shown in Table I and the fault tree and event tree shown in Figure 4 and Figure 5, respectively, are used as inputs in the risk calculation.

Table V and Figure 9 present the results of the optimization carried out using Dakota. Table V presents the capital cost and risk of the safety system before and after the design optimization. The table shows that the optimal design has a capital cost of around $83 million, which is about a $16 million reduction from the capital cost of the initial, unoptimized design of the GNF safety system. The design optimization resulted in a 16% reduction in the capital cost of the GNF, while meeting the safety goals of the GNF.

Panels a and b of Figure 9 present the median fragilities and capital costs, respectively, of individual SSCs. These panels show that most of the cost reductions in the optimized design are from the nuclear and steam supply system (NSSS) components – steam generator, reactor vessel, coolant pump, and piping – as their corresponding median fragilities are reduced in the optimization process. Panel c of the figure presents the risk contributions of individual minimal cutsets (i.e., possible accident sequences) of the safety system. Panel c shows that, in spite of a reduction in their median fragilities, the risk contributions from the cutsets corresponding to the NSSS components (the four cutsets from the right) are reduced in the optimized design. This is because the CRDM, which accompanies all the other NSSS components in their minimal cutsets, is strengthened significantly in the optimized design (see panel a). Since the occurrence of these minimal cutsets requires both the CRDM and an NSSS component to fail, the strengthening of CRDM and the consequent reduction in its failure probability results in a net reduction in the risk contribution of the corresponding cutsets. Note that the steam generator, reactor vessel, coolant pump, and piping are all relatively expensive components compared to the CRDM. Therefore, instead of strengthening all of these expensive components the design optimization algorithm automatically prioritizes strengthening the CRDM for a lower cost, resulting in a lower overall capital cost. In this idealized and illustrative safety system, the CRDM can be considered as providing a redundancy for the rest of the NSSS components since, according to the fault tree in Figure 4, failure of any of the NSSS components needs the CRDM to also fail to result in system failure. However, note that in real nuclear safety systems, the CRDM provides a different function of reactivity control and shutdown of the system.

Panel b of Figure 9 also shows that another source of cost reduction is the structure, which is the most expensive SSC in the safety system. However, this is a smaller reduction than that seen in the NSSS components and is achieved by reducing the median fragility, which consequently increases the structure's risk contribution by more than 50%. Unlike the structure, the battery, which is much less expensive than the structure, is strengthened in the optimized design and consequently, its risk contribution decreases by 30%. There are two takeaways from this observation. First, the risk contributions of the structure and the battery are much more sensitive to changes in fragility than that of the NSSS components. This is because of the added redundancy in the NSSS components provided by the CRDM, which acts as another layer of defense for the NSSS systems. Unlike these components, the structure and the battery do not have any redundancy, that is, the failure of the structure or the battery will inevitably lead to the failure of the safety system[b]. Second, due to the sensitivity of the change in fragilities in the structure and the battery, their fragilities and costs are adjusted only marginally by the optimization algorithm, when compared to the reactor vessel, coolant pump, and piping. This shows that the optimization process rewards redundancies and leverages them to reduce the total capital cost of the system.

Table V: Capital cost and risk of the safety system before and after design optimization

	Capital cost (USD millions)	**Seismic risk**
Initial	99.2	5.2×10^{-5}
Optimized	83.2	4.9×10^{-5}

[b] It must be noted that in practice, nuclear systems have a range of redundancies and typically do not have single points of failure such as the idealized safety system here. Such a fault tree is chosen here to demonstrate the importance of redundancies on the capital cost.

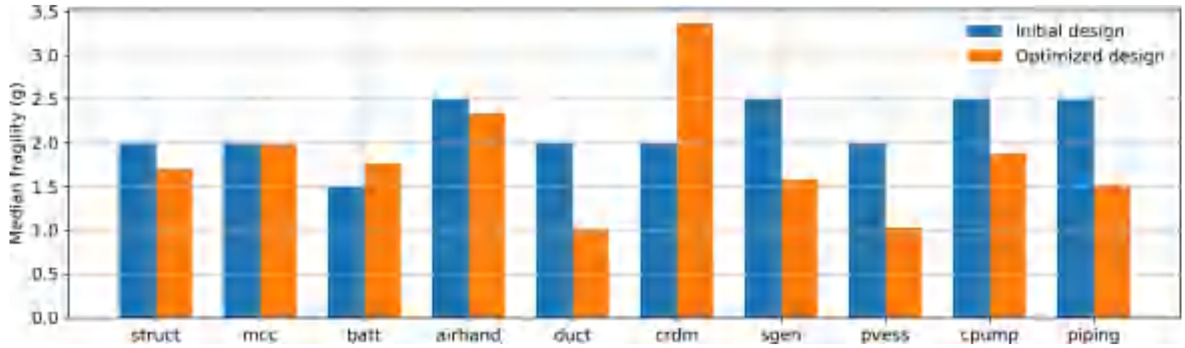

a. Median fragilities

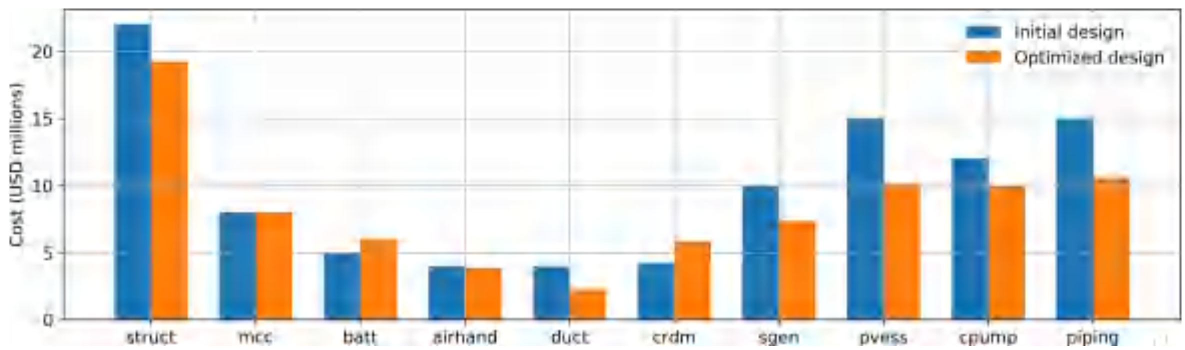

b. Capital cost of individual SSCs

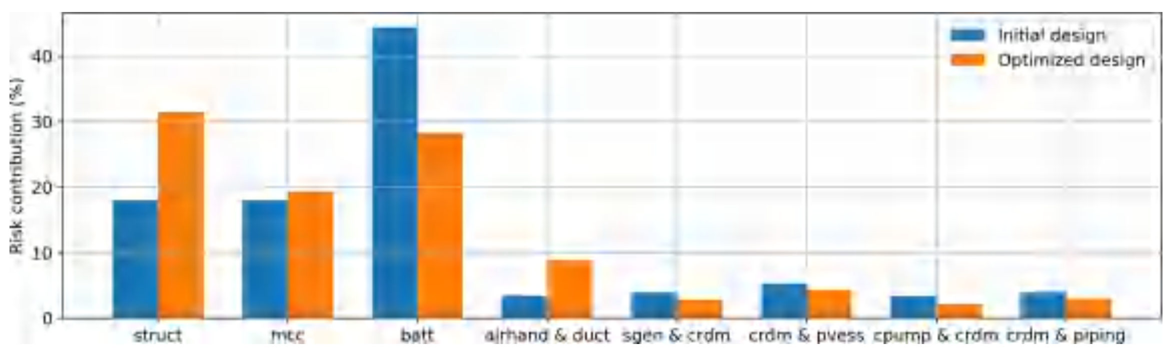

c. Risk contribution from the minimal cutsets

Figure 9: Comparison between initial and optimized design of the GNF safety system

V.C.1 Effect of cost functions on the optimized design

The data on seismic design penalty is scarce, especially for advanced nuclear reactor components and it can be challenging to build accurate cost functions for any SSC. However, design optimization is typically performed during the preliminary design stage when the design is 'fine-tuned' before being detailed. Therefore, approximate cost functions are usually adequate, as long as the *trends* of the costs are modeled, especially the rate of increase of seismic design costs with increase in the median fragility (or other measures of seismic integrity), relative rate of increase amongst different SSCs, and the relative cost of individual SSCs. For example, since the structure is the most expensive SSC of the GNF safety system and has a considerable contribution to the total seismic risk, even small changes in the rate of increase might considerably affect the total capital cost. On the contrary, since the duct is relatively less expensive and has a small contribution to the risk, the change in the cost function of the duct may not affect the optimized design significantly.

In order to examine the effect of cost functions on the optimized design, a separate design optimization is performed in this section with modified cost functions presented in Figure 10. These cost functions are modified such that the total initial capital cost is almost the same, but the rate of increase of the capital cost is modified for all components, except for the duct and air handler. The initial design of the system, that is, the median fragilities of the SSCs are kept unchanged. A higher rate of capital cost increase indicates a larger seismic design penalty for the component. Figure 10 shows that the rate is increased for MCC, battery, and CRDM, whereas it is reduced for the structure, and the rest of the NSSS components, coolant pump, reactor vessel, steam generator, and piping. These modifications are intended to counter the design changes made by the optimization algorithm in the previous section, where the costs and median fragilities of the NSSS components and the structure are reduced, whereas battery and CRDM are strengthened and their capital costs are increased. With the modified cost functions, a reduction in the median fragilities of the structure and the NSSS components will not reduce the cost as much, and an increase in the median fragility of the MCC, battery, and CRDM will result in a larger increase in the cost than those from the original cost functions.

The initial and optimized capital cost and seismic risk with the modified cost functions are presented in Table VI below. The table shows that the seismic risk is unchanged from that calculated using the original cost functions (see Table V) which is expected since the median fragilities are also unchanged. Whereas the initial capital cost is similar to that calculated from the original cost functions, the optimized capital cost is considerably larger. With the modified cost functions, the optimal capital cost is around $88.5 million, which is about a 10% reduction from the initial capital cost. In contrast the design optimization with the original cost functions resulted in a 16% reduction in the capital cost. Figure 11 presents the median fragilities, costs, and risk contributions, calculated for the initial and optimized design with the modified cost functions. Although the total cost reduction is smaller, note that the trends in the cost reduction (or increase) amongst various SSCs are almost the same as those calculated using the original cost functions. Panels a and b of Figure 11 show that the median fragilities and the costs of the structure, and the NSSS components are decreased during the optimization, and those of the battery and CRDM are increased. However, the magnitudes of these increases and decreases are smaller than those calculated using the original cost functions. For example, the median fragility of the CRDM is increased by about 70% with the original cost functions, but it increases by less than 50% with the modified cost functions since they have a higher rate of cost increase, which indicates that it is more expensive to strengthen the CRDM. These observations indicate that the relative costs of the SSCs, rate of change of the costs with median capacity, and relative risk contributions of the individual SSCs can have a considerable effect on the results of the design optimization.

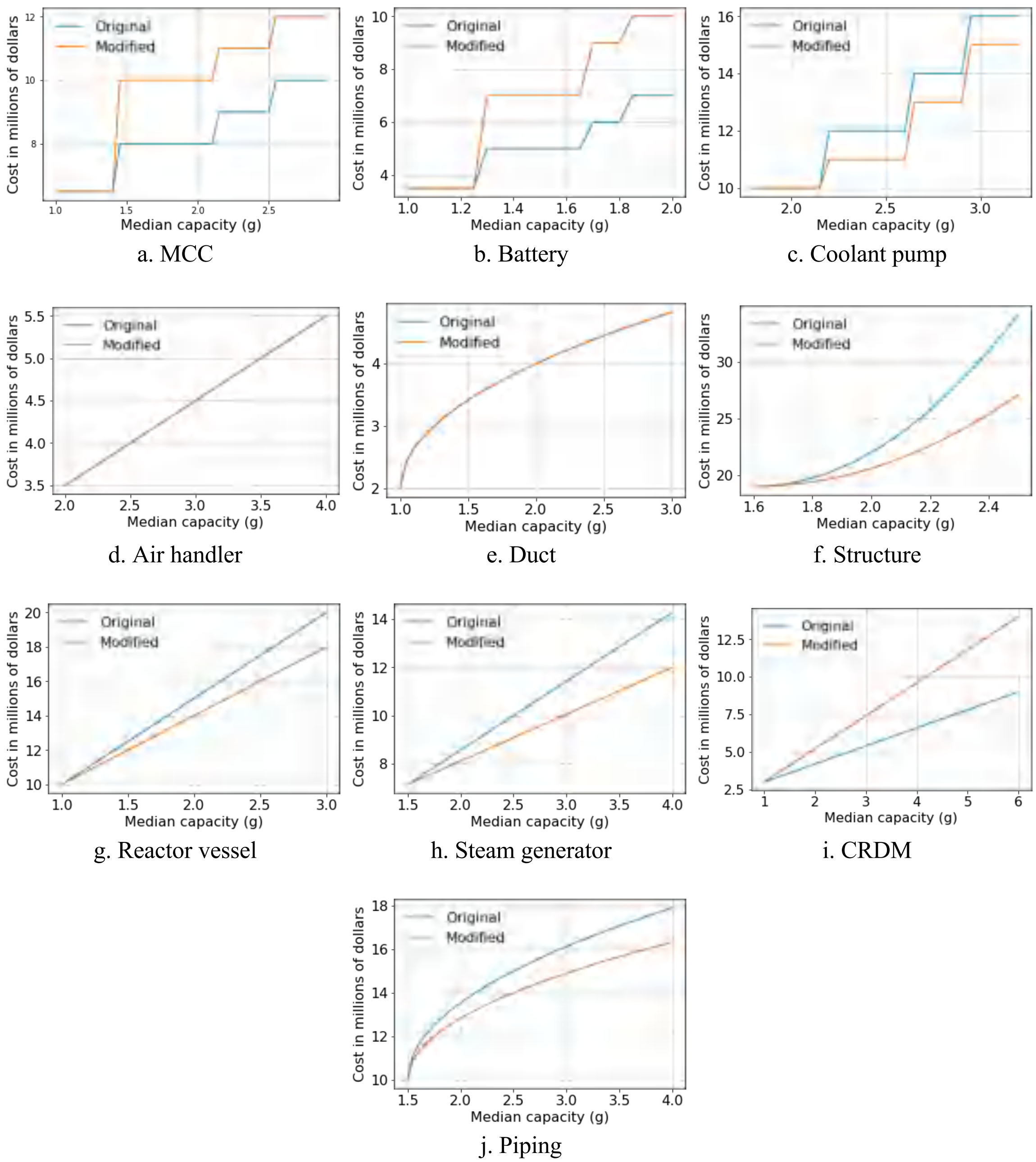

a. MCC

b. Battery

c. Coolant pump

d. Air handler

e. Duct

f. Structure

g. Reactor vessel

h. Steam generator

i. CRDM

j. Piping

Figure 10: Modified cost functions

Table VI: Capital cost and risk from optimization using modified cost functions from Figure 10

	Capital cost (USD millions)	Seismic risk
Initial	98.6	5.2×10^{-5}
Optimized	88.5	5.0×10^{-5}

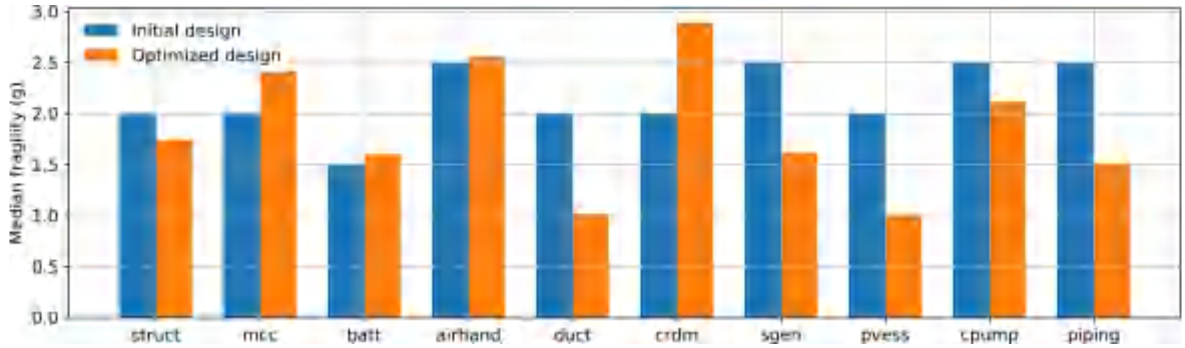

a. Median fragilities

b. Capital cost of individual SSCs

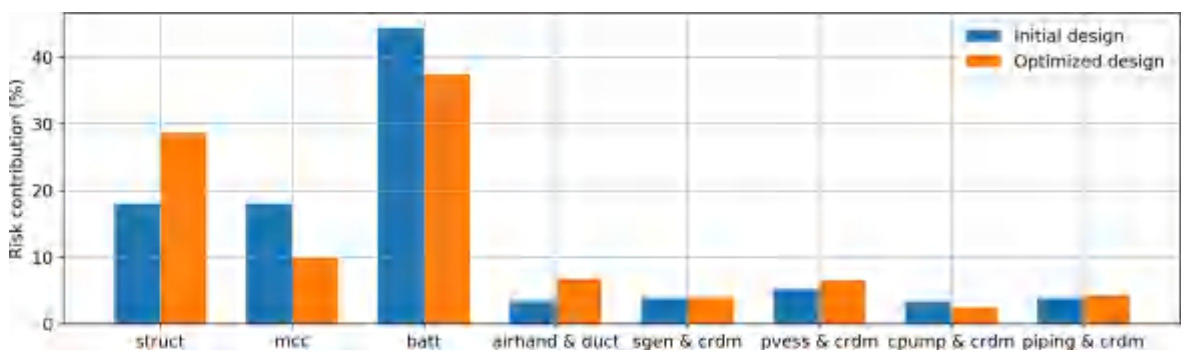

c. Risk contribution from the minimal cutsets

Figure 11: Comparison between initial and optimized designs with modified cost functions

V.D Design optimization with component seismic isolation

Similar to seismic base isolation, component seismic isolation involves the use of seismic isolators for individual SSCs to drastically reduce their seismic demands. The choice of selecting the SSCs to seismically isolate in a nuclear power plant depends on various factors including the seismic hazard, cost penalty for their seismic design, cost of seismically isolating the SSC, risk contribution of the SSC, etc. This section demonstrates the use of the design optimization procedure to choose the optimal set of SSCs, which, if seismically isolated, will result in a minimal capital cost. The optimization process developed in the previous sections is extended to include component seismic isolation for this purpose.

Equations 3 and 4 present the objective function and the constraints, respectively of the optimization problem when component seismic isolation is included. Similar to equation 1, the objective function (i.e., the total capital cost), C', is a sum of the cost functions, ${c'}_i$, evaluated at the values of the design variables. The design variables here include a_i and si_i, which are the median seismic fragility and a Boolean variable, respectively, corresponding to an SSC, i. The Boolean variable takes the value of 0 when the SSC is not seismically isolated, and a value of 1 when it is seismically isolated. The cost functions of the individual SSCs, ${c'}_i$, are equal to the original cost functions from Figure 7, if the SSC is not seismically isolated. The cost of an isolated SSC is evaluated as a fraction of the nominal capital cost of the SSC (i.e., when it is not designed for seismic loads), which is assumed to be the cost evaluated at the lower bound (l_i) of its fragility range. This cost is given by $\alpha c_i(l_i)$ as shown in equation 3, where α is termed as the isolation cost ratio. Seismic isolation typically results in a drastic reduction in seismic demands and the seismic risk[13]. Therefore, seismically isolated SSCs are assumed to have a negligible contribution to the system seismic risk. Additionally, the isolation system itself is assumed to have a high enough seismic fragility to not make a significant contribution to the total seismic risk. In order to ensure that the risk contribution of isolated SSCs is almost zero, their median fragilities are scaled up by a factor of 20 during the evaluation of the system risk, R'. The rest of the parameters of equations 3 and 4 are identical to those in equations 1 and 2, and are described in Section III.

$$C'(a_1, a_2, .. a_n, si_1, si_2, .. si_n) = \sum_{i=1}^{n} {c'}_i(a_i, si_i)$$

$${c'}_i(a_i, si_i) = \begin{cases} \alpha c_i(l_i)\ if\ si_i = 1 \\ c_i(a_i)\ if\ si_i = 0 \end{cases} \tag{3}$$

$$\text{minimize } C'(a_1, a_2,\ ..\ a_n, si_1, si_2, .. si_n)$$

$$\text{subject to the constraints}\begin{cases} R'(LN(a_1,\beta_1),LN(a_2,\beta_2),\ ..\ LN(a_n,\beta_n)\,) \le \mathrm{R_U} \\ l_1 \le\ a_1 \le\ u_1 \\ l_2 \le\ a_2 \le\ u_2 \\ .. \\ l_n \le\ a_n \le\ u_n \\ si_i \in \{0,1\} \end{cases} \tag{4}$$

The data for seismic isolation cost of specific SSCs is not available in the literature since component isolation is yet to be adopted in nuclear power plants. When available, component seismic isolation cost will likely depend on the component itself, its support structures, and the seismic hazard at the site of the facility. For the study in this section, a value of 0.1 is assumed for the isolation cost ratio, α, which implies that the isolation cost of the SSC is 10% of the nominal capital cost of the SSC. This value is likely conservative, since Yu, et al.[13] estimate that when base isolation is used, the capital cost of the SSCs increases by only 1% of the nominal capital cost for a facility that is similar to that considered in this study and designed for the same seismic hazard. However, a value of 0.1 is still deemed adequate the purpose of the demonstration of the design optimization algorithm in this section. The same value of α is used for all SSCs for simplicity.

Seismic isolation may not be possible for all SSCs. For example, distributed systems like piping cannot be seismically isolated, at least in a traditional sense, using commonly used isolation systems such as elastomeric or sliding bearings. Systems, structures, and components like the CRDM may not be independent components but a part of other SSCs like the reactor vessel, based on the design of the reactor. Additionally, isolating the containment structure (referred to as 'structure' in this study) independently may not be possible for some reactors without compromising its containment function (e.g., light water reactors), unless the whole facility is base isolated, which is not the focus of this study. In order to replicate these practical limitations in the design optimization of the safety system, it is assumed that the seismic isolation is not admissible for piping, duct, CRDM, and the structure, and only the rest of the SSCs can be isolated. This limitation is enforced in Dakota by setting the Boolean variable, si_i, to be 0 (i.e., not seismically isolated) for piping, duct, CRDM, and the structure, and allowing the algorithm to choose between 0 and 1 for the rest of the SSCs.

Table VII presents the capital cost and seismic risk of the initial, unoptimized design (which has no seismic isolation) and the optimized design when component seismic isolation is included in the optimization process. The table shows that design optimization with component seismic isolation results in a capital cost of \$78.6 million, which is about a \$21 million smaller than the initial capital cost and about \$5 million smaller than the optimized capital cost when component seismic isolation is not considered (see Table V). Including component seismic isolation for the GNF safety system therefore results in about a 21% reduction in capital cost, which is 5% additional reduction from the optimized design when seismic isolation is not included.

Figure 12 presents the median fragilities (panel a), capital costs (panel b) of each SSC, and a breakdown of the risk amongst the various minimal cutsets (panel c) for the initial and optimized designs. In panel a, if an SSC is seismically isolated in the optimized design, the corresponding median fragility is not presented since it is assumed to be a large number. Therefore, from panel a, it can be inferred that the optimized design requires the MCC, battery, air handler, and reactor vessel to be seismically isolated. (Note that seismic isolation is inadmissible for the piping, duct, CRDM, and the structure.) Panel c shows that the cutsets involving isolated SSCs have almost zero risk contributions, which is expected since the isolated SSCs have are assumed to have a large median fragility and have a tiny probability of failure. For the other, non-isolated components, the figure shows that the median fragilities are reduced from their corresponding initial values, resulting in a net reduction in the capital cost. Panel c also shows that the seismic risk of the optimized system is distributed amongst the non-isolated systems, thereby increasing their risk contributions. While this is a consequence of using an idealized safety system with only 10 SSCs, concentration of the risk in a small subset of the SSCs may not be a preferred result in practice. Such a risk concentration can be avoided by setting risk constraints on individual SSCs, which is possible when using genetic algorithms.

Table VII: Capital cost and seismic risk from optimization including seismic isolation

	Capital cost (USD millions)	**Seismic risk**
Initial	99.2	5.2 x 10^{-5}
Optimized	78.6	4.9 x 10^{-5}

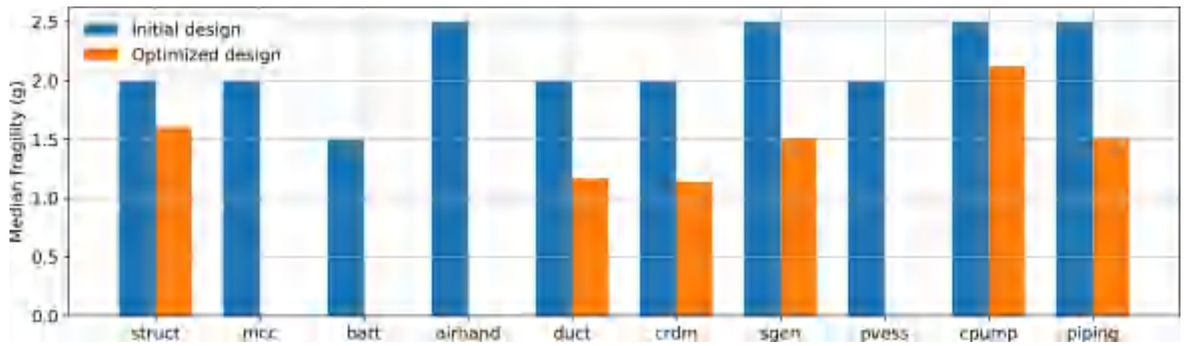

a. Median fragilities

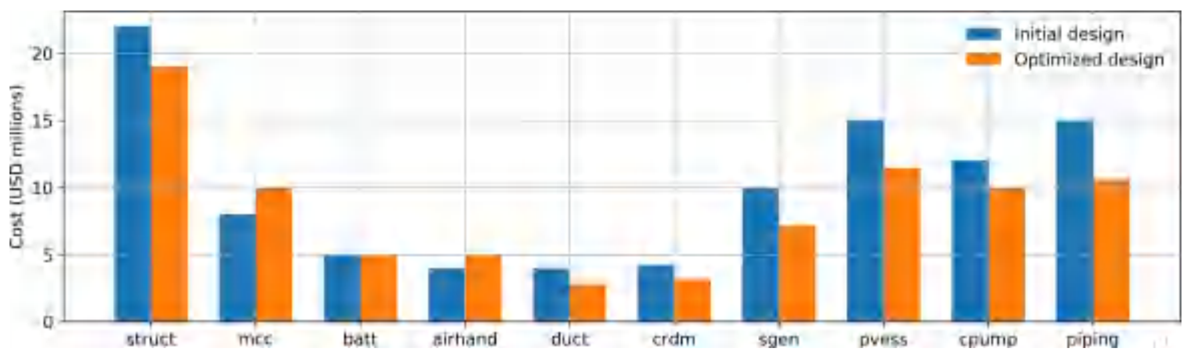

b. Capital cost of individual SSCs

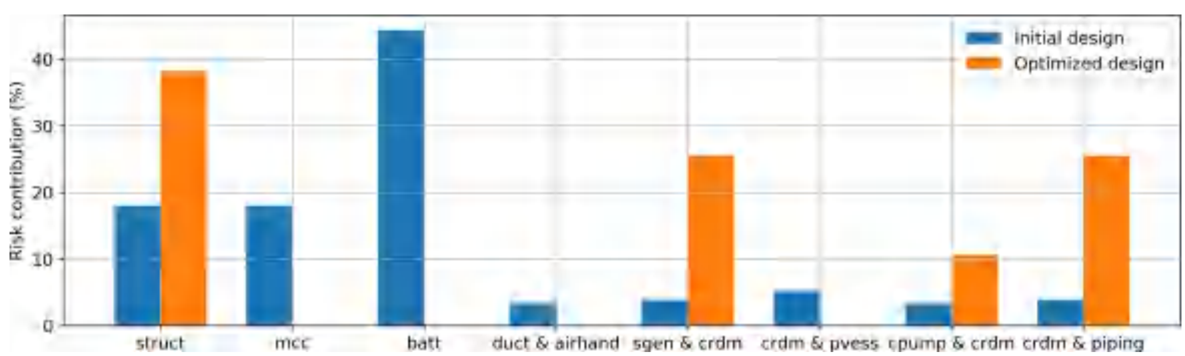

c. Risk contribution from the minimal cutsets

Figure 12: Comparison of initial and optimized designs of the GNF safety system while considering component seismic isolation

V.D.1 Impact of component seismic isolation on N^{th}-of-a-kind (NOAK) design

In the previous section, the benefit of seismic isolation is quantified in terms of reduction in capital cost of first-of-a-kind (FOAK) components as the seismic demand on the SSC is significantly reduced. The capital cost of a FOAK component includes the costs of seismic analysis, design, qualification, regulatory review, and first-time tooling and fabrication. If seismically isolated, the required seismic capacity of the FOAK component will be reduced to its nominal level (i.e., assumed to be the cost at the lower bound fragility for this study) but there is an additional cost to isolate (assumed arbitrarily to be 10% of the nominal cost in the previous section). The costs for FOAK analysis, design, qualification, and regulatory review of isolated components are expected to be substantially smaller than their non-isolated counterparts, but are assumed to be identical for this exercise. The cost of NOAK components is expected to be smaller than FOAK components with improvements in fabrication methods, a larger and more efficient nuclear supply chain, and investments in advanced manufacturing. Without seismic isolation, such cost reduction in NOAK components is likely marginal since the components must still be analyzed, designed, and qualified for each site and facility. If seismically isolated, much greater cost reductions are possible with NOAK-isolated equipment because standardized, off-the-shelf equipment could be used, assuming seismic isolation will reduce the design seismic demand to below the nominal level, and the cost of seismic analysis, design, and qualification should be eliminated. (Importantly, the time required to execute these preparatory activities is eliminated, resulting in significant additional cost savings, which are not quantified here.) Lal et al.[15] and EPRI[31] conducted a survey among nuclear equipment designers and manufacturers and show that such preparatory costs are significant, and similar to the FOAK fabrication cost of the SSCs. This implies that without the seismic design, analysis and qualification costs, the nominal capital cost of the NOAK components will likely be much smaller (less than one-half) than that of the FOAK components considered in their study. This section examines the impact of isolated NOAK component cost on the optimized capital cost of the GNF. Assuming that the nominal cost of the NOAK component is halved (decreased by 50%) and isolation increases the capital cost by 10%, an α value of -0.4 is used for the isolated components in this section. The same value of α is again used for all components.

Table VIII presents the capital cost and seismic risk of the safety system with the initial design and the optimized design with FOAK (α = 0.1) and NOAK (α = -0.4) seismic isolation cost. The results for the original, FOAK seismic isolation cost are taken from Table VII. Table VIII shows that for NOAK designs, the optimized capital cost is about \$60 million, which is a 40% reduction from the unoptimized capital cost and also significantly smaller than the optimized cost when component seismic isolation is considered for FOAK design. Figure 13 presents the median fragilities (panel a) and capital costs (panel b) of the individual SSCs, and a breakdown of the system risk amongst various cutsets (panel c). The figure shows that all the SSCs that could be seismically isolated are isolated in the optimized design. The only SSCs that are not isolated are the SSCs that are assumed to be non-conducive to seismic isolation: structure, duct, CRDM, and piping. This is an expected result since a negative value of α reduces the SSC cost to below the nominal value while the risk is also reduced significantly. Panel a shows that the fragilities of the non-isolated components are also reduced in the optimized design, indicating that isolating all the other components provides a significant risk margin that is leveraged in the non-isolated components. Panel c shows that the seismic risk in the optimized design is distributed among just two minimal cutsets. Similar to that observed in panel c of Figure 12, this result is not preferred in practice and can be avoided by setting more SSC specific risk constraints in the optimization process. The results of this section show that the benefits of seismic isolation are a lot more apparent when NOAK costs are considered and therefore, the impact of seismic isolation is greatest when the economic benefits of standardization are taken into account.

Table VIII: Capital cost and seismic risk from optimization with seismic isolation of an NOAK design

	Capital cost (USD millions)	Seismic risk
Initial	99.2	5.2×10^{-5}
Optimized (α = 0.1)	78.6	4.9×10^{-5}
Optimized (α = -0.4)	60.0	3.1×10^{-5}

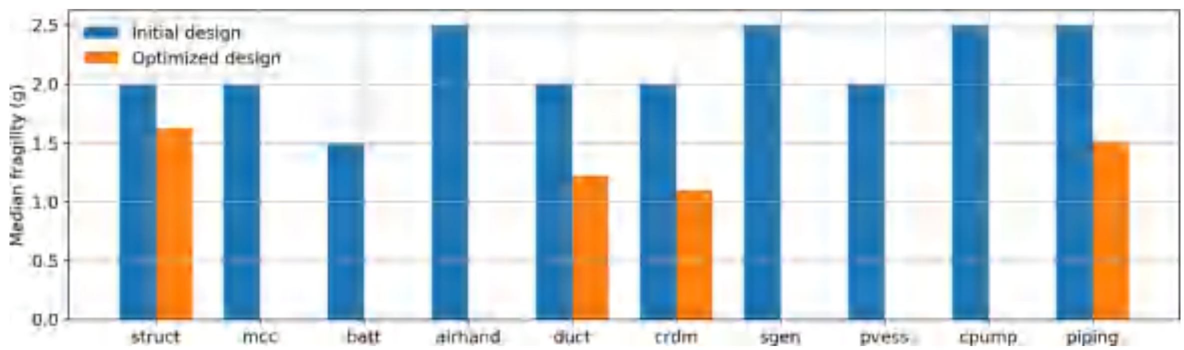

a. Median fragilities

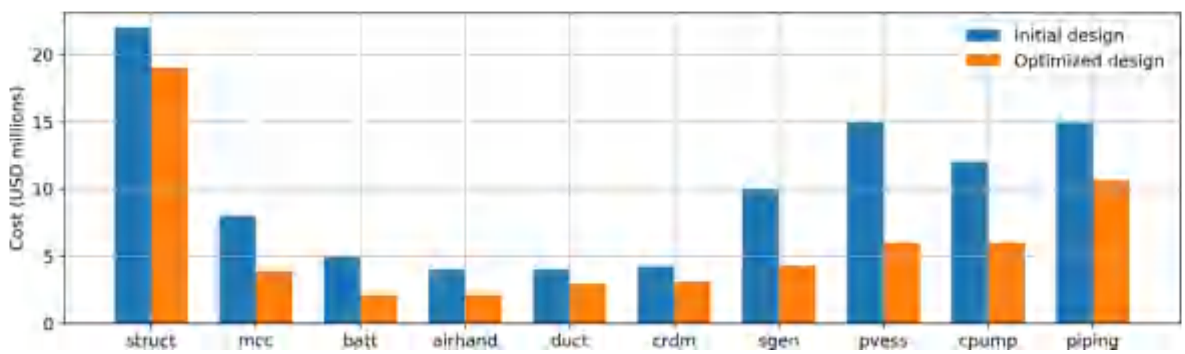

b. Capital cost of individual SSCs

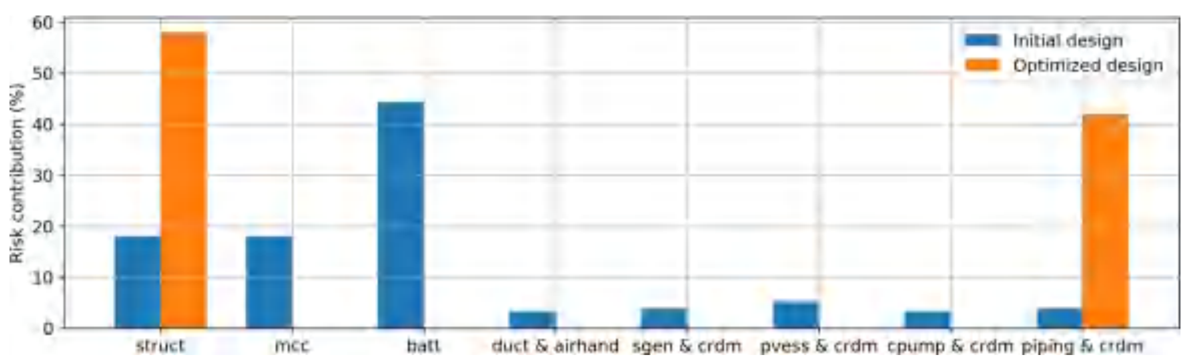

c. Risk contribution from the minimal cutsets

Figure 13: Comparison of initial and optimized designs of the GNF safety system with seismic isolation of an NOAK design

VI SUMMARY AND IMPLEMENTATION IN PRACTICE

This paper presents the development and demonstration of a risk- and cost-based seismic design optimization methodology for application to safety-related nuclear structures including nuclear power plants. The methodology is demonstrated on a generic nuclear facility (GNF) that houses a safety system that performs the function of containing radioactive materials within the facility. The safety system is representative of both current and advanced nuclear power plants and comprises three classes of components: (1) electrical components including the motor control center and battery, (2) containment components including the containment structure, air handler, and duct, and (3) nuclear and steam supply systems (NSSS) including the reactor vessel, steam generator, coolant pump, and piping. The GNF is assumed to be sited at the Idaho National Laboratory (INL) site, which has a low-to-moderate seismic hazard. The design of the GNF is characterized by the seismic fragilities of its SSCs that represent their seismic integrity. A representative fault tree and event tree are developed to describe the accident sequences of the GNF. The initial fragility functions (median and lognormal standard deviation) are generic and chosen from the EPRI SPRA guide. The fragility ranges for the design optimization, are also taken from this guide. Given the lack of data to relate the capital costs of SSCs to their seismic capacities, generic cost functions are developed for the SSCs. These cost functions represent the seismic design ‘penalty’ that is, the additional costs required to strengthen the SSC or its support to achieve the required seismic capacity. With the initial fragilities and cost functions, the total capital cost of the unoptimized design of the GNF is around $99.2 million. Risk assessment is performed using MASTODON and the seismic risk from the initial design is calculated to be around 5.2×10^{-5}. Design optimization is performed using a genetic algorithm in Dakota, with the dual goals of minimizing overnight capital cost and meeting safety performance goals. The performance goal of the GNF is to not exceed a seismic risk of 5.0×10^{-5}, which is input as a constraint to the genetic algorithm. Design optimization is performed with and without considering seismic isolation of individual SSCs as a design option. Results of the design optimization include the capital cost and seismic risk of the optimized GNF design, and the corresponding design variables, that is, median seismic fragilities and the set of seismically isolated SSCs. From the optimized design, the final capital cost of each SSC, and the risk contribution of each minimal cut set are also calculated. For each design optimization case, a comparison of these results is presented between the initial (unoptimized) and optimized design.

The design optimization process developed and demonstrated in this paper presents designers with an ‘intelligent finetuning’ tool and enables them to evaluate the optimal use of technologies such as seismic isolation. In its current form, the design optimization process is not intended to replace the current, code-based design procedures, but it can be used to augment these deterministic design procedures and improve the design in its early stages. The results of the optimization framework can be improved by using more accurate cost functions and a more comprehensive SPRA, as more information is available during the design process. While the structural response evaluation was not considered in this study for simplicity, designers can include it in the SPRA process as described in Section II. Including the structural response evaluation can be computationally intensive, but the computational effort can be reduced using statistical tools such as surrogate models, or even low-fidelity, fast-running numerical models. Additionally, the response evaluations can be performed only when the capacities are changed beyond a certain extent and it can be assumed that the structural response does not change significantly for small changes in the SSC capacity. As the optimization process is implemented in practice, better results can also be achieved by improving the SPRA models such as by accounting for structural response correlations between different SSCs or incorporating the seismic fragility of the isolation systems. The design optimization process presented in this paper can also be extended in the future to be integrated with the newly developed and LMP and RIPB processes which will likely greatly influence the way advanced reactors are designed for seismic loads.

VII CONCLUSIONS

The following conclusions can be drawn from this paper:

1. The results of Section V.B show that, although heuristically based, genetic algorithms exhibit convergence and stability and often provide an optimal solution, even for discontinuous and non-differentiable objective functions. Given this versatility and robustness of genetic algorithms, the optimization framework developed here can be scaled and modified to design optimization in practice, which involve more complex cost functions and variables (e.g., Boolean variables such as those used for component seismic isolation), much larger fragility ranges, and numerous design constraints. Additionally, while genetic algorithms are not guaranteed to provide a mathematical optimum, they to provide a design solution that is much better than the initial design and satisfies the design constraints. Genetic algorithms are therefore well suited for the large-scale seismic design optimization of nuclear facility safety systems.
2. Design optimization of the GNF ignoring seismic isolation resulted in a 16% reduction in capital cost while meeting the safety goals. This is a significant reduction and demonstrates that 'fine-tuning' a design can result in large capital cost savings. A comparison of the costs and risk contributions corresponding to the initial and optimized design shows that the optimization algorithm automatically rewards redundancy in design and defense-in-depth. Additionally, the algorithm ensures that the cost profile of the facility aligns with the risk profile, that is, the cost investment is prioritized for SSCs that most contribute to the risk and provide the largest benefit-cost ratio. Results from a separate design optimization using modified cost functions shows that moderate changes in the cost functions (such as increasing the rate of change of the cost) can affect the total optimized cost, but not significantly.
3. Including component seismic isolation in the FOAK design optimization resulted in a 5% additional cost reduction with a total cost reduction of 21% and a new optimized capital cost of $78 million. This optimization is performed with an assumption that the seismic isolation cost is about 10% of the nominal cost of the SSC, which is likely high. The results of the optimization showed that the fragility of all the SSCs is either reduced or the SSC is seismically isolated. A separate optimization considering cost reductions from seismic isolation in an NOAK design in

which, standardized, off-the-shelf equipment are be used, resulted in an optimized capital cost of $60 million, which is a significant reduction from the capital cost of the unoptimized design. This demonstration shows that considering the impact of standardization is crucial in understanding the benefits of seismic isolation and that these benefits, when combined with those from design optimization, will be quite significant in NOAK designs.

4. In cases with and without seismic isolation, changing the cost functions (or reducing the isolation cost ratio to model the reduction in seismic design, analysis, and qualification in standardized, NOAK components) resulted in considerable changes in the optimized design. However, the choices of using design optimization or using component seismic isolation themselves are more significant in terms of cost reduction than using accurate cost functions or isolation cost ratios. Although using accurate cost estimates might provide more confidence in the cost of the optimized design, cost functions that reasonably capture the (a) relative costs of the SSCs and (b) rate of change of the cost with median fragility are likely adequate to provide a design that is better than the initial design. The design optimization process presented in this paper should therefore be viewed as an intelligent alternative to manual 'fine-tuning', which is typically performed for a preliminary design. Given that accurate cost functions or the seismic design penalties for advanced reactor SSCs may not be available for some time, estimates like those calculated by Lal et al.[14,15] and Electric Power Research Institute[31], are adequate to optimize nuclear power plant designs and minimize capital costs.
5. Design optimization of nuclear power plants is possible and can result in significant capital cost reduction without compromising safety. The optimization framework developed here is versatile and scalable and can be extended to real facilities when the required data is available. The framework can be extended to include component seismic isolation, which results in additional cost reductions. In practice, cost reductions due to seismic isolation can be significant, especially since it enables the use of off-the-shelf components eliminates the SSC qualification costs and the corresponding engineering and design costs and potentially accelerates the regulatory process.

ACKNOWLEDGMENTS

This study was funded by the Department of Energy through Office of Technology Transitions (OTT) and the Office of Nuclear Energy (NE), Southern Nuclear Development Company, X-Energy, and TerraPower. The project participants included Jason Redd from Southern Nuclear Development Company, Paul Kirchman and Harlan Bowers from X-Energy, Michael Cohen and Kevin Kramer from TerraPower, and Sai Sharath Parsi and Kaivalya Lal from the University at Buffalo, State University of New York. The contributions of the project team and the financial support from the various agencies is gratefully acknowledged. The authors also acknowledge the anonymous reviewers, whose feedback and suggestions have improved the quality of this paper.

REFERENCES

1 J. BUONGIORNO, J. PARSONS, M. CORRADINI, and D. PETTI, "The Future of Nuclear Energy in a Carbon Constrained World - An Interdisciplinary MIT Study," 2018, MIT Energy Initiative, Massachusetts Institute of Technology, Cambridge, MA, USA.

2 K. DAWSON and P. SABHARWALL, "A Review of Light Water Reactor Costs and Cost Drivers," 2017, Idaho National Laboratory, INL/EXT-17-43273, Idaho Falls, ID.

3 K. GOGAN and E. INGERSOLL, "The ETI Nuclear Cost Drivers Project: Summary Report," 2018, Energy Technologies Institute (ETI), Loughborough, UK.

4 R. J. BUDNITZ and M. W. MIELER, "Towards a More Risk-Informed and Performance-Based Framework for the Regulation of the Seismic Safety of Nuclear Power Plants," 2016, U.S. Nuclear Regulatory Commission, NUREG/CR-7214, Washington, DC.

5 AMERCIAN SOCIETY OF CIVIL ENGINEERS, "Seismic Design Criteria for Structures, Systems, and Components in Nuclear Facilities," 2019, American Society of Civil Engineers (ASCE), ASCE 43–19, Reston, VA.

6 N. CHOKSHI, R. J. BUDNITZ, M. K. RAVINDRA, B. DASGUPTA, J. STAMATAKOS, and O. PENSADO, "A Proposed Alternative Risk-Informed and Performance-Based Regulatory Framework for Seismic Safety at NRC Regulated Facilities - Task 3 (Draft)," 2020, Southwest Research Institute (SwRI).

7 NUCLEAR ENERGY INSTITUTE, "Risk-Informed Performance-Based Technology Inclusive Guidance for Non-Light Water Reactor Licensing Basis Development," 2019, Nuclear Energy Institute (NEI), NEI-18-04 Revision 1, Washington, D.C.

8 USNRC, "Guidance For A Technology-inclusive, Risk-informed, And Performance-based Methodology To Inform The Licensing Basis And Content Of Applications For Licenses, Certifications, And Approvals For Non-light-water Reactors " 2020, United States Nuclear Regulatory Commission, Regulatory Guide 1.233 Revision 0, Washington, D.C.

9 G. SCHUMOCK, S. ZHANG, P. FARSHADMANESH, J. G. OWENS, N. KASZA, J. STEARNS, T. SAKURAHARA, and Z. MOHAGHEGH, "Integrated Risk-Informed Design (I-RID) Methodological Framework and Computational Application for FLEX Equipment Storage Buildings of Nuclear Power Plants," Progress in Nuclear Energy **120** (2020).

10 J. WANG and M. LIN, "Seismic Probabilistic Risk Assessment and Application in a Nuclear Power Plant," Nuclear Technology **203**, pp. 221-231 (2018).

11 S. KWAG and D. HAHM, "Multi-Objective-Based Seismic Fragility Relocation for a Korean Nuclear Power Plant," Natural Hazards **103**, pp. 3633-3659 (2020).

12 J. D. STEVENSON, "Historical Development of the Seismic Requirements for Construction of Nuclear Power Plants in the U.S. and Worldwide and their Current Impact on Cost and Safety," presented at the Structural Mechanics and Reactor Technology (SMiRT 17), Prague, Czech Republic, 2003.

13 C.-C. YU, C. BOLISETTI, J. L. COLEMAN, B. KOSBAB, and A. S. WHITTAKER, "Using Seismic Isolation to Reduce Risk and Capital Costs of Safety-Related Nuclear Facilities," Nuclear Engineering and Design **326**, pp. 268-284 (2018).

14 K. LAL, S. S. PARSI, H. CHARKAS, K. SHIRVAN, M. COHEN, P. KIRCHMAN, B. KOSBAB, and A. WHITTAKER, "Reducing the Capital Cost of Nuclear Power Plants Using Seismic Isolation," presented at the International Congress on Advances in Nuclear Power Plants (ICAPP), Abu Dhabi, UAE, 2020.

15 K. LAL, S. S. PARSI, D. SCOTT, K. SHIRVAN, M. COHEN, P. KIRCHMAN, B. KOSBAB, and A. WHITTAKER, "Cost Basis for Utilizing Seismic Isolation in Nuclear Power Plants," presented at the Structural Mechanics in Reactor Technology (SMiRT 25), Charlotte, NC, USA, 2019.

16 Y.-N. HUANG, A. S. WHITTAKER, and N. LUCO, "Performance Assessment of Conventional and Base-Isolated Nuclear Power Plants for Earthquake and Blast Loadings," 2008, Multidisciplinary Center for Earthquake Engineering Research, MCEER-08-0019, University at Buffalo, The State University of New York, Buffalo, NY.

17 S. VEERARAGHAVAN, C. BOLISETTI, A. SLAUGHTER, J. COLEMAN, S. DHULIPALA, W. HOFFMAN, K. KIM, E. KURT, R. SPEARS, and L. MUNDAY, "MASTODON: An Open-Source Software for Seismic Analysis and Risk Assessment of Critical Infrastructure," Nuclear Technology (2020).

18 P. VAISHNAV, S. S. BODDA, and A. GUPTA, "Instruction Manual for SPRA Integration in MASTODON," 2021, Idaho National Laboratory, INL/EXT-21-61991, Idaho Falls, Idaho.

19 B. M. ADAMS, L. E. BAUMAN, W. J. BOHNHOFF, K. R. DALBEY, M. S. EBEIDA, J. P. EDDY, M. S. ELDRED, P. D. HOUGH, K. T. HU, J. D. JAKEMAN, J. A. STEPHENS, L. P. SWILER, D. M. VIGIL, and T. M. WILDEY, "Dakota - A Multilevel Parallel Object-Oriented Framework for Design Optimization, Parameter Estimation, Uncertainty Quantification, and Sensitivity Analysis: Version 6.0 User’s Manual," 2014, Sandia National Laboratory, SAND2014-4633.

20 ELECTRIC POWER RESEARCH INSTITUTE, "Seismic Probabilistic Risk Assessment Implementation Guide," 2013, Electric Power Research Institute (EPRI), EPRI Report 3002000709, Palo Alto, CA.

21 T. Y. YANG, J. P. MOEHLE, B. STOJADINOVIC, and A. DER KIUREGHIAN, " Performance Evaluation of Structural Systems: Theory and Implementation," Journal of Structural Engineering **135** (10), 1146-1154 (2009).

22 Y. N. HUANG, A. S. WHITTAKER, and N. LUCO, "A Probabilistic Seismic Risk Assessment Procedure for Nuclear Power Plants: (I) Methodology," Nuclear Engineering and Design **241**, pp.3996-4003 (2011).

23 UNITED STATES NUCLEAR REGULATORY COMMISSION, "Systems Analysis Programs for Hands-on Integrated Reliability Evaluations (SAPHIRE)," 2011, United States Nuclear Regulatory Commission (USNRC), Washington, District of Columbia.

24 C. L. SMITH and T. L. WOOD, "Systems Analysis Programs for Hands-on Integrated Reliability Evaluations (SAPHIRE) Version 8," 2011, U.S. Nuclear Regulatory Commission, NUREG/CR-7039, Idaho Falls, ID, USA.

25 J. B. FUSSEL and W. E. VESELY, "A New Methodology for Obtaining Cut Sets for Fault Trees," Transactions of the American Nuclear Society **15** (1) (1972).

26 C. BOLISETTI, W. HOFFMAN, S. S. PARSI, K. J. KRAMER, P. KIRCHMAN, J. REDD, J. COLEMAN, and A. S. WHITTAKER, "Risk- and Cost-Based Seismic Design Optimization of Advanced Nuclear Reactor Systems", in *25th International Conference on Structural Mechanics in Reactor Technology (SMiRT25)* (Charlotte, NC, 2019).

27 J. E. EDDY and K. LEWIS, "Effective Generation of Pareto Sets Using Genetic Programming," presented at the ASME Design Engineering Technical Conference, 2001.

28 S. S. RAO, *Engineering Optimization - Theory and Practice (4th Edition)*. (2009), John Wiley & Sons.

29 C. BOLISETTI, C. YU, J. L. COLEMAN, B. KOSBAB, and A. S. WHITTAKER, "Characterizing the Benefits of Seismic Isolation for Nuclear Structures: A Framework for Risk-Based Decision Making," 2016, Idaho National Laboratory, INL/EXT-16-40122, Idaho Falls, Idaho.

30 J. D. STEVENSON, "Evaluation of the Cost Effects on Nuclear Power Plant Construction Resulting from the Increase in Seismic Design Level," 1981, U. S. Nuclear Regulatory Commission, NUREG/CR-1508, Washington, D. C.

31 ELECTRIC POWER RESEARCH INSTITUTE, "Cost Basis for Utilizing Seismic Isolation for Nuclear Power Plant Design," 2020, Electric Power Research Institute, EPRI Report 03002018345, Charlotte, NC.